

Research Article

Piyapan Suwattananuruk, Jutamas Jiaranaikulwanitch*, Pornthip Waiwut, Opa Vajragupta

Lead discovery of a guanidinylyl tryptophan derivative on amyloid cascade inhibition

<https://doi.org/10.1515/chem-2020-0067>

received February 11, 2020; accepted April 3, 2020

Abstract: Amyloid cascade, one of pathogenic pathways of Alzheimer's disease (AD), was focused as one of drug discovery targets. In this study, β -secretase (BACE1) inhibitors were designed aiming at the development of multifunctional compounds targeting amyloid pathogenic cascade. Tryptophan was used as a core structure due to its properties of the central nervous system (CNS) penetration and BACE1 inhibition activity. Three amino acid residues and guanidine were selected as linkers to connect the tryptophan core structure and the extended aromatic moieties. The distance between the aromatic systems of the core structure and the extended moieties was kept at the optimal length for amyloid- β ($A\beta$) peptide binding to inhibit its fibrillation and aggregation. Sixteen designed compounds were evaluated *in silico*. Eight hit compounds of TSR and TGN series containing serine and guanidine linkers, respectively, were identified and synthesized based on docking results. **TSR2** and **TGN2** were found to exert strong actions as BACE1 (IC_{50} 24.18 μ M and 22.35 μ M) and amyloid aggregation inhibitors (IC_{50} 37.06 μ M and 36.12 μ M). Only **TGN2** demonstrated a neuroprotective effect in SH-SY5Y cells by significantly reducing $A\beta$ -induced cell death at a concentration of 2.62 μ M. These results support the validity of multifunctional approaches to inhibition of the β -amyloid cascade.

* **Corresponding author: Jutamas Jiaranaikulwanitch**, Center of Excellence for Innovation in Drug Design and Discovery and Department of Pharmaceutical Chemistry, Faculty of Pharmacy, Mahidol University, Bangkok 10400, Thailand; Innovation Center for Holistic Health, Nutraceuticals, and Cosmeceuticals, Faculty of Pharmacy, Chiang Mai University, Chiang Mai 50200, Thailand; Department of Pharmaceutical Sciences, Faculty of Pharmacy, Chiang Mai University, Chiang Mai 50200, Thailand, e-mail: jutamas.jia@cmu.ac.th, tel: +66 5394438

Piyapan Suwattananuruk, Opa Vajragupta: Center of Excellence for Innovation in Drug Design and Discovery and Department of Pharmaceutical Chemistry, Faculty of Pharmacy, Mahidol University, Bangkok 10400, Thailand

Pornthip Waiwut: Faculty of Pharmaceutical Sciences, Ubon Ratchathani University, Ubon Ratchathani 34190, Thailand

Keywords: tryptophan, multifunction activities, beta-secretase inhibitor, amyloid aggregation inhibition, neuroprotection

1 Introduction

Alzheimer's disease (AD) is currently the most common neurodegenerative disorder, particularly affecting aged members of society and causing impairments of cognition and memory. Two pathological features, amyloid- β ($A\beta$) plaques and neurofibrillary tangles, have been found in the brains of patients with AD. The observation of these proteins led to the development of drugs for AD, which obstruct the production of $A\beta$ and neurofibrillary tangles and their neurotoxic cascades [1,2]. In the etiology of $A\beta$, the β -secretase enzyme (BACE1) is an attractive drug target as it generates $A\beta$ peptide, the main constituent of toxic $A\beta$ oligomers and plaques [3–5]. Decreased $A\beta$ production would obstruct $A\beta$ oligomerization and consequently reduce $A\beta$ aggregation. A number of BACE1 inhibitors and amyloid aggregation inhibitors have been developed as single target drugs but more than half have apparently failed in clinical trials. Only two BACE1 inhibitors are currently in phase III clinical trials and three compounds in phase II clinical trials [6]. The use of a multitarget single ligand is one of the most challenging approaches to AD drug discovery, aiming to reduce the late-stage clinical attrition. This new paradigm has gained popularity because it suits the complex etiology and multiple pathogenic mechanisms involved in AD [7–9].

However, ligand developed to be AD drug should be considered about the possibility to enter the CNS. Three methods of molecule entering to brain are passive diffusion, active transport via solute carrier (SLC) superfamily, and endocytosis [10]. Thus, the objective of this research was to design and synthesize novel BACE1 inhibitors with multifunctional actions including anti-amyloid aggregation and antioxidant properties by using *in silico* hit screening and finding. Tryptophan was used as a core structure to make a molecule to transport into CNS.

2 Materials and methods

2.1 *In silico* study

Molecular dockings were performed to determine the binding mode of compounds to BACE1 and A β using the AutoDock program suite, version 4.2. The Pymol program was used to visualize the generated docking graphics objects. The 3D-structures of the compounds were generated and optimized with ChemDraw Ultra 12.0 and Chem3D Ultra 12.0.

The protein template preparation and docking parameters using in this research were the same as in previous study [11]. Briefly, the BACE1 template 2IRZ-F constructed from the crystal structures of 2IRZ [12] and 1FKN [13] was used as a BACE1 macromolecule. The docking parameters in the *in silico* studies for BACE1 were as follows: 100 runs of the genetic algorithm (GA), a population size of 150, 1,50,00,000 energy evaluations per run, and a maximum number of generations of 27,000.

A β template, 1Z0Q-1, was constructed from X-ray crystal structures of inhibitor-bound A β (PDB code: 1Z0Q) [14]. Docking parameters in the *in silico* studies for A β binding were as follows: 100 runs of the GA, a population size of 150, 50,00,000 energy evaluations per run, and a maximum number of generations of 27,000.

2.2 Synthesis part

Chemical reagents were purchased from Acros, Aldrich, or AK Science. Melting points were determined on a Model 9100 melting point apparatus (Electrothermal, UK). IR spectra were recorded using a Nicolet FTIR Instruments machine (ThermoFisher, USA). Nuclear magnetic resonance (NMR) spectra were recorded using Bruker Fourier 300 MHz spectrometers (Bruker, Switzerland) with tetramethylsilane as an internal standard. Mass spectra (MS) were obtained in positive ESI mode (Bruker, Switzerland). The ^1H and ^{13}C -NMR spectra of synthesized compounds were shown in the supplemental materials (Figures S1–S20).

2.2.1 General synthesis procedure of TSR1–TSR4

A solution of compound **T2** (1 mmol), $\text{NH}_2\text{-R}_2$ (1 mmol), HBTU (1.5 mmol), and DIPEA (3 mmol) in 5 mL of DMF was stirred at room temperature. After 18 h stirring,

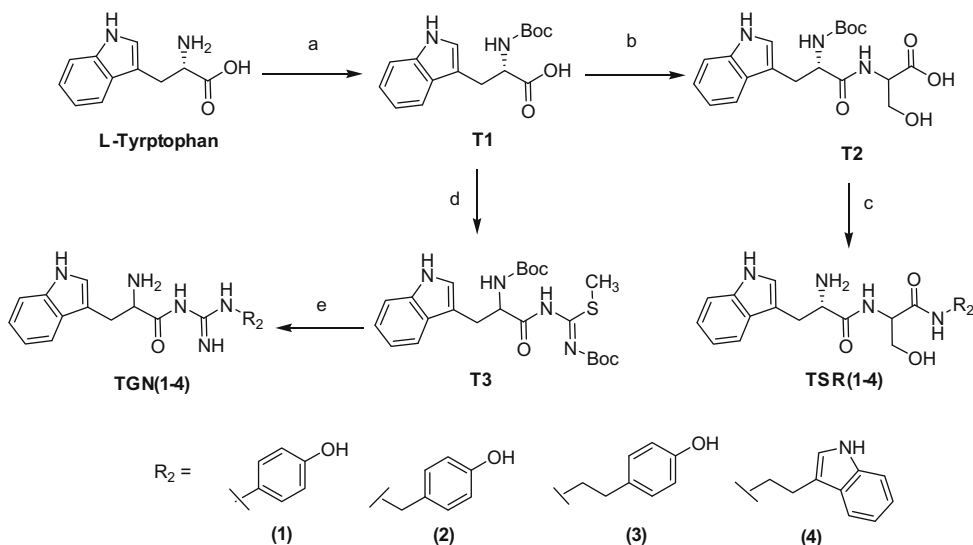
water was added. The aqueous phase was extracted with ethyl acetate. The organic extracts were combined and dried. The obtained residue was purified by column chromatography on silica gel to yield compound **Boc-TSR1** to **Boc-TSR4**. The protecting group of the obtained compound was removed by 50% of TFA in ethyl acetate at room temperature for 3 h. The reaction mixture was adjusted to pH 7 by saturated sodium bicarbonate solution and extracted with ethyl acetate. The combined organic layers were dried. The residue was purified by column chromatography on silica gel to yield **TSR1–TSR4** (Scheme 1).

2.2.2 (*S*)-2-Amino-*N*-((*S*)-3-hydroxy-1-((4-hydroxyphenyl)amino)-1-oxopropan-2-yl)-3-(1*H*-indol-3-yl)propanamide (TSR1)

Compound **Boc-TSR1** was purified by column chromatography on silica gel ($\text{CHCl}_3/\text{EtOAc}/\text{NH}_4\text{OH}$ 7:3:0.01) to yield white powder. Compound **TSR1** was purified by column chromatography on silica gel ($\text{CHCl}_3/\text{EtOAc}/\text{MeOH}$ 4:5:1) to yield yellow solid (hygroscopic). Yield 261.45 mg (68.37%). FTIR (ATR, ν , cm^{-1}): 3,392–3,155 (O–H, N–H), 3,110 (sp^2 C–H), 2,927 (sp^3 C–H), 1,674, 1,514 (C=O, C=C) 1,457, 1,444 (C–C), 1,368 (C–O), 1,201, 1,146 (C–N, C–O). ^1H -NMR spectrum in DMSO-d_6 (δ , ppm): 10.88 (s, 1H, indole-NH), 9.73 (s, 1H, OH), 8.20 (s, 1H, NHa), 7.38 (s, 1H, NHb), 7.57 (d, 1H, J 8.0 Hz, 1H, H9'), 7.34 (d, 1H, J 8.1 Hz, H6'), 7.38 (d, 2H, J 8.9 Hz, H2'', 6''), 7.20 (s, 1H, H4'), 7.05 (t, 1H, J 8.1 Hz, H7'), 6.96 (t, 1H, J 7.9 Hz, H8'), 6.69 (d, 2H, J 8.8 Hz, H3'', H5''), 3.88 (dd, 1H, J_1 6.0 Hz, J_2 7.3 Hz, H1'), 3.64 (m, 3H, H2, H4a, H4b), 3.19 (dd, 1H, J_1 5.8 Hz, J_2 14.6, H2b'), 3.02 (dd, 1H, J_1 7.2 Hz, J_2 14.6 Hz, H2a'). ^{13}C -NMR spectrum in DMSO-d_6 (δ , ppm): 174.9 (C1), 168.7 (C3), 153.9 (C4''), 136.7 (C5'), 130.9 (C1''), 130.9 (C2'', C6''), 127.9 (C10'), 124.3 (C4''), 121.6 (C7'), 118.9 (C9'), 118.7 (C8'), 115.4 (C3'', C5''), 111.8 (C6'), 110.9 (C3'), 62.4 (C1'), 55.6 (C4), 55.6 (C2), 31.1 (C2'). HRMS (ESI) m/z : 405.1532 [M + Na].

2.2.3 (*S*)-2-Amino-*N*-((*S*)-3-hydroxy-1-((4-hydroxybenzyl)amino)-1-oxopropan-2-yl)-3-(1*H*-indol-3-yl)propanamide (TSR2)

Compound **Boc-TSR2** was purified by column chromatography on silica gel ($\text{CHCl}_3/\text{EtOAc}/\text{Hex}$ 4:5:1) to yield white powder. Compound **TSR2** was purified by column chromatography on silica gel ($\text{CHCl}_3/\text{EtOAc}/\text{MeOH}/4:4:1$) to yield white solid (hygroscopic). Yield 216.25 mg



Scheme 1: The scheme of synthesis of compounds in the TSR and TGN series: (a) Boc₂O, NaOH, THF/H₂O (1:1), rt, 18 h; (b) (i) L-serine methyl ester hydrochloride, HBTU, DIPEA, DMF, rt, 18 h, (ii) MeOH, KOH, rt, 3 h; (c) (i) NH₂-R₂, HBTU, DIPEA, DMF, rt, 18 h, (ii) TFA:EtOAc (1:1), rt, 3 h; (d) *N*-*tert*-butoxycarbonyl (Boc)-protected 2-methyl-2-thiopseudourea (1a), HATU, NMM, DMF, rt, 18 h; and (e) (i) NH₂-R₂, HATU, NMM, DMF, rt, 18 h, (ii) TFA:EtOAc (1:1), rt, 1.5 h.

(54.55%). FTIR (ATR, ν , cm⁻¹): 3,419–3,184 (O–H, N–H), 3,110 (sp² C–H), 2,925 (sp³ C–H), 1,667, 1,516 (C=O, C=C), 1,455, 1,435 (C–C), 1,361, 1,337 (C–O), 1,228, 1,192, 1,131 (C–N, C–O). ¹H-NMR spectrum in DMSO-d₆ (δ , ppm): 10.96 (s, 1H, indole-NH), 8.45 (s, 1H, OH), 8.26 (t, 1H, *J* 5.9 Hz, NH), 7.98 (t, 1H, *J* 5.9 Hz, NH), 7.62 (d, 1H, *J* 7.8 Hz, H9'), 7.35 (d, 1H, *J* 7.7 Hz, H6'), 7.20 (s, 1H, H4'), 7.07 (t, 1H, *J* 7.8 Hz, H7'), 7.05 (d, 2H, *J* 8.5 Hz, H2'', H6''), 6.97 (t, 1H, *J* 7.6 Hz, H8'), 6.70 (dd, 2H, *J*₁ 8.4 Hz, *J*₂ 8.4 Hz, H3'', H5''), 4.18 (d, 2H, *J* 5.6 Hz, H7''), 3.80 (dd, 1H, *J*₁ 5.1 Hz, *J*₂ 7.6 Hz, H1'), 3.72 (dd, 1H, *J*₁ 4.9 Hz, *J*₂ 5.6 Hz, H2), 3.63 (dd, 1H, *J*₁ 5.5 Hz, *J*₂ 10.9 Hz, H4b), 3.51 (dd, 1H, *J*₁ 5.0 Hz, *J*₂ 10.9 Hz, H4a), 3.17 (dd, 1H, *J*₁ 5.1 Hz, *J*₂ 14.1 Hz, H2b'), 2.94 (dd, 1H, *J*₁ 7.7 Hz, *J*₂ 14.0 Hz, H2a'). ¹³C-NMR spectrum in DMSO-d₆ (δ , ppm): 175.5 (C1), 170.2 (C3), 156.7 (C4''), 136.7 (C5'), 129.7 (C1''), 128.7 (C2'', C6''), 127.8 (C10'), 124.9 (C4'), 121.4 (C7'), 118.9 (C9'), 118.8 (C8'), 115.4 (C3'', C5''), 111.9 (C6'), 109.3 (C3'), 62.1 (C1'), 55.6 (C4), 54.5 (C2), 42.1 (C7''), 29.6 (C2'). HRMS (ESI) *m/z*: 419.1687 [M + Na].

2.2.4 (S)-2-Amino-N-((S)-3-hydroxy-1-(4-hydroxyphenethyl)amino)-1-oxopropan-2-yl)-3-(1H-indol-3-yl)propanamide (TSR3)

Compound **Boc-TSR3** was purified by column chromatography on silica gel (CHCl₃/EtOAc/Hex 4:5:1) to yield white powder. Compound **TSR3** was purified by column

chromatography on silica gel (CHCl₃/EtOAc/MeOH 4:4:1) to yield yellow solid (hygroscopic). Yield 170.09 mg (41.14%). FTIR (ATR, ν , cm⁻¹): 3,413–3,184 (O–H, N–H), 3,116 (sp² C–H), 2,927 (sp³ C–H), 1,667, 1,515 (C=O, C=C), 1,454, 1,435 (C–C), 1,361, 1,340 (C–O), 1,227, 1,202, 1,136 (C–N, C–O). ¹H-NMR spectrum in DMSO-d₆ (δ , ppm): 10.90 (s, 1H, indole-NH), 9.18 (s, 1H, OH), 8.17 (s, 1H, NH), 7.83 (t, 1H, *J* 7.56 Hz, NH), 7.58 (d, 1H, *J* 7.4 Hz, H9'), 7.35 (d, 1H, *J* 7.3 Hz, H6'), 7.21 (d, 1H, *J* 2.2 Hz, H4'), 6.99 (d, 2H, *J* 8.3 Hz, H2'', H6''), 7.07 (t, 1H, *J* 7.0 Hz, H7'), 6.98 (t, 1H, *J* 7.0 Hz, H8'), 6.67 (d, 2H, *J* 8.4 Hz, H3'', H5''), 3.64 (dd, 1H, *J*₁ 5.2 Hz, *J*₂ 7.7 Hz, H1'), 3.55 (dd, 1H, *J*₁ 5.4 Hz, *J*₂ 10.9 Hz, H4b), 3.40 (dd, 1H, *J*₁ 4.8 Hz, *J*₂ 10.9 Hz, H4a), 3.12 (m, 4H, H2b', H2, H8''), 2.85 (dd, 1H, *J*₁ 7.9 Hz, *J*₂ 14.4 Hz, H2a'), 2.57 (t, 2H, *J* 7.9 Hz, H7''). ¹³C-NMR spectrum in DMSO-d₆ (δ , ppm): 174.4 (C1), 170.2 (C3), 156.1 (C4''), 136.7 (C5'), 129.9 (C2'', C6''), 129.9 (C1''), 127.8 (C10'), 124.5 (C4'), 121.4 (C7'), 118.9 (C9'), 118.7 (C8'), 115.6 (C3'', C5''), 111.8 (C6'), 110.6 (C3'), 62.2 (C1'), 55.4 (C4), 55.3 (C2), 41.2 (C8''), 34.8 (C7''), 30.7 (C2'). HRMS (ESI) *m/z*: 433.1840 [M + Na].

2.2.5 (S)-N-(2-(1H-Indol-2-yl)ethyl)-2-((S)-2-amino-3-(1H-indol-3-yl)propanamido)-3-hydroxypropanamide (TSR4)

Compound **Boc-TSR4** was purified by column chromatography on silica gel (CHCl₃/EtOAc/Hex 4:5:1) to yield

white powder. Compound **TSR4** was purified by column chromatography on silica gel (CHCl₃/EtOAc/MeOH 4:4:1) to yield yellow solid (hygroscopic). Yield 260.36 mg (60.06%). FTIR (ATR, ν , cm⁻¹): 3,392–3,216 (O–H, N–H), 3,113 (sp² C–H), 2,919 (sp³ C–H), 1,659, 1,516 (C=O, C=C) 1,457, 1,433 (C–C), 1,363, 1,336 (C–O), 1,229, 1,202, 1,180 (C–N, C–O). ¹H-NMR spectrum in DMSO-d₆ (δ , ppm): 10.81 (s, 2H, indole-NH), 7.87 (m, 2H, NH, NH), 7.60 (d, 1H, *J* 7.6 Hz, H7''), 7.53 (d, 1H, *J* 7.7 Hz, H9'), 7.32 (d, 1H, *J* 8.0 Hz, H6', H4''), 7.15 (m, 2H, H4', H2''), 7.05 (t, 2H, *J* 7.4 Hz, H8', H6''), 6.97 (t, 2H, *J* 7.3 Hz, H7', H5''), 4.24 (m, 2H, H1', H2), 3.60 (dd, 1H, *J* 9.9 Hz, H4b), 3.50 (dd, 1H, *J*₁ 5.7 Hz, *J*₂ 10.8 Hz, H4a), 3.09 (dd, 1H, *J*₁ 4.7 Hz, *J*₂ 14.2 Hz, H2b'), 2.94 (m, 1H, H2a'), 2.76 (m, 4H, H9'', H10''). ¹³C-NMR spectrum in DMSO-d₆ (δ , ppm): 175.1 (C1), 170.3 (C3), 136.9 (C3''), 136.7 (C5'), 127.9 (C8''), 127.6 (C10'), 123.2 (C2''), 123.0 (C4'), 121.6 (C5''), 121.4 (C7'), 118.9 (C9', C7''), 118.7 (C8', C6''), 112.0 (C4''), 111.8 (C6'), 111.0 (C1''), 110.8 (C3'), 62.3 (C1'), 55.7 (C4), 55.1 (C2), 44.9 (C10''), 31.2 (C9''), 26.1 (C2'). HRMS (ESI) *m/z* 434.2193 [M + H].

2.2.6 General synthesis procedure of TGN1–TGN4

A solution of compound **T3** (1 mmol), NH₂-R₂ (1 mmol), HATU (1.5 mmol), and *N*-methylmorpholine (NMM) (3 mmol) in 5 mL of DMF was stirred at room temperature. After 18 h stirring, water was added. The aqueous phase was extracted with ethyl acetate. The combined organic extracts were dried. The obtained residue was purified by column chromatography on silica gel to yield compound **Boc-TGN1** to **Boc-TGN4**. The protecting group of the obtained compound was removed by 50% of TFA in ethyl acetate at room temperature for 1.5 h. The reaction mixture was adjusted to pH 7 by saturated sodium bicarbonate solution and extracted with ethyl acetate. The combined organic layers were dried. The residue was purified by column chromatography on silica gel to yield **TGN1–TGN4** (Scheme 1).

2.2.7 (S)-2-Amino-N-(N-(4-hydroxyphenyl)carbamimidoyl)-3-(1H-indol-3-yl)propanamide (TGN1)

Compound **Boc-TGN1** was purified by column chromatography on silica gel (EtOAc/CHCl₃/Hex 2:7:1) to yield white powder. Compound **TGN1** was purified by column chromatography on silica gel (CHCl₃/EtOAc/MeOH 6:3:1) to yield white powder. Yield 190.75 mg (56.54%); m.p. = 208 (d) °C. FTIR (ATR, ν , cm⁻¹): 3,417–3,018 (O–H, N–H), 3,080 (sp² C–H), 2,923 (sp³ C–H), 1,678, 1,588, 1,511

(C=O, C=C, C=N), 1,456, 1,432 (C–C), 1,366, 1,341 (C–O st), 1,204, 1,139 (C–N). ¹H-NMR spectrum in DMSO-d₆ (δ , ppm): 10.85 (s, 1H, indole-NH), 9.36 (s, 1H, OH), 8.26 (s, 1H, NH), 7.57 (d, 1H, *J* 7.6 Hz, H9'), 7.52 (s, 1H, NH), 7.34 (s, 1H, NH), 7.34 (d, 1H, *J* 7.7 Hz, H6'), 7.35 (d, 2H, *J* 8.9 Hz, H2'', H6''), 7.21 (d, 1H, *J* 2.2 Hz, H4'), 7.06 (t, 1H, *J* 7.5 Hz, H7'), 6.97 (t, 1H, *J* 7.4 Hz, H8'), 6.70 (dd, 2H, *J* 8.8 Hz, H3'', H5''), 4.05 (m, 1H, H1'), 3.16 (dd, 1H, *J*₁ 4.1 Hz, *J*₂ 14.6 Hz, H2b'), 2.93 (dd, 1H, *J*₁ 6.1 Hz, *J*₂ 14.6 Hz, H2a'). ¹³C-NMR spectrum in DMSO-d₆ (δ , ppm): 171.8 (C1), 158.5 (C2), 154.5 (C4''), 136.4 (C5'), 129.9 (C1''), 128.1 (C2'', C6''), 127.9 (C10'), 123.9 (C4'), 121.2 (C7'), 119.1 (C9'), 118.6 (C8'), 115.8 (C3'', C5''), 111.7 (C6'), 110.0 (C3'), 60.8 (C1'), 27.4 (C2'). HRMS (ESI) *m/z*: 360.1426 [M + Na].

2.2.8 (S)-2-Amino-N-(N-(4-hydroxybenzyl)carbamimidoyl)-3-(1H-indol-3-yl)propanamide (TGN2)

Compound **Boc-TGN2** was purified by column chromatography on silica gel (EtOAc/CHCl₃/Hex 2:7:1) to yield white powder. Compound **TGN2** was purified by column chromatography on silica gel (CHCl₃/EtOAc/MeOH 2:7:1) to yield brown viscous (hygroscopic). Yield 487.40 mg (53.33%). FTIR (ATR, ν , cm⁻¹): 3,394–3,111 (O–H, N–H), 3,065 (sp² C–H), 2,925 (sp³ C–H), 1,674, 1,611, 1,515 (C=O, C=C, C=N) 1,456, 1,431 (C–C), 1,357, 1,338 (C–O), 1,201, 1,136 (C–N). ¹H-NMR spectrum in DMSO-d₆ (δ , ppm): 10.87 (s, 1H, indole-NH), 9.32 (s, 1H, OH), 8.10 (s, 1H, NH), 7.55 (s, 1H, NH), 7.55 (d, 1H, *J* 7.7 Hz, H9'), 7.34 (s, 1H, NH), 7.34 (d, 1H, *J* 7.6 Hz, H6'), 7.13 (s, 1H, H4'), 6.93 (d, 2H, *J* 8.4 Hz, H2'', H6''), 7.06 (t, 1H, *J* 7.5 Hz, H7'), 6.97 (t, 1H, *J* 7.5 Hz, H8'), 6.67 (d, 2H, *J* 8.4 Hz, H3'', H5''), 4.24 (m, 2H, H7''), 4.06 (m, 1H, H1'), 3.14 (dd, 1H, *J*₁ 4.0 Hz, *J*₂ 14.6 Hz, H2b'), 2.83 (dd, 1H, *J*₁ 6.9 Hz, *J*₂ 14.6 Hz H2a'). ¹³C-NMR spectrum in DMSO-d₆ (δ , ppm): 171.9 (C1), 156.9 (C4''), 156.8 (C2), 136.5 (C5'), 129.1 (C1''), 128.9 (C2'', C6''), 127.9 (C10'), 123.9 (C4'), 121.2 (C7'), 119.0 (C9'), 118.7 (C8'), 115.5 (C3'', C5''), 111.7 (C6'), 110.3 (C3'), 61.4 (C1'), 45.0 (C7''), 27.9 (C2'). HRMS (ESI) *m/z*: 374.1590 [M + Na].

2.2.9 (S)-2-Amino-N-(N-(4-hydroxyphenethyl)carbamimidoyl)-3-(1H-indol-3-yl)propanamide (TGN3)

Compound **Boc-TGN3** was purified by column chromatography on silica gel (EtOAc/CHCl₃/EtOAc 2:7:1) to yield white powder. Compound **TGN3** was purified by column chromatography on silica gel (CHCl₃/EtOAc/MeOH 3:6:1) to yield yellow viscous (hygroscopic). Yield 266.68 mg (62.03%). FTIR (ATR, ν , cm⁻¹): 3,387–3,120 (O–H, N–H),

3,056 (sp² C–H), 2,925 (sp³ C–H), 1,694, 1,612, 1,514 (C=O, C=C, C=N) 1,455, 1,434 (C–C), 1,362, 1,338 (C–O), 1,230, 1,131 (C–N). ¹H-NMR spectrum in DMSO-d₆ (δ, ppm): 11.01 (s, 1H, indole-NH), 9.22 (s, 1H, OH), 7.96 (t, 1H, *J* 5.6 Hz, NH), 7.68 (s, 2H, NH, NH), 7.68 (d, 1H, *J* 7.8 Hz, H9'), 7.37 (d, 1H, *J* 7.8 Hz, H6'), 7.23 (d, 1H, *J* 2.3 Hz, H4'), 7.09 (t, 1H, *J* 7.8 Hz, H7'), 7.00 (d, 2H, *J* 8.4 Hz, H2'', H6'') 7.02 (t, 1H, *J* 7.5 Hz, H8'), 6.68 (d, 2H, *J* 8.5 Hz, H3'', H5''), 4.03 (m, 1H, H1'), 3.22 (m, 3H, H2b', H8''), 3.05 (dd, 1H, *J*₁ 8.2 Hz, *J*₂ 14.7 Hz, H2a') 2.58 (t, 2H, *J* 7.5 Hz, H7''). ¹³C-NMR spectrum in DMSO-d₆ (δ, ppm): 172.6 (C1), 156.3 (C2), 156.2 (C4''), 136.5 (C5'), 129.9 (C1''), 129.9 (C2'', C6''), 127.9 (C10'), 123.7 (C4'), 121.3 (C7'), 118.9 (C9'), 118.7 (C8'), 115.6 (C3'', C5''), 111.7 (C6'), 110.6 (C3'), 66.8 (C8''), 61.4 (C1'), 28.8 (C7''), 27.9 (C2'). HRMS (ESI) *m/z*: 388.1737 [M + Na].

2.2.10 (S)-N-(N-(2-(1H-Indol-2-yl)ethyl)carbamimidoyl)-2-amino-3-(1H-indol-3-yl)propanamide (TGN4)

Compound **Boc-TGN4** was purified by column chromatography on silica gel (EtOAc/CHCl₃/EtOAc 2:7:1) to yield white powder. Compound **TGN4** was purified by column chromatography on silica gel (CHCl₃/EtOAc/MeOH 3:6:1) to yield white viscous (hygroscopic). Yield 154.22 mg (39.70%). FTIR (ATR, ν, cm⁻¹): 3298.97 (N–H), 3,084 (sp² C–H), 2,924 (sp³ C–H), 1,670, 1,612, 1,494 (C=O, C=C, C=N) 1,455, 1,431 (C–C), 1,359, 1,339 (C–O), 1,201, 1,135 (C–N). ¹H-NMR spectrum in DMSO-d₆ (δ, ppm): 10.98, 10.91 (s, 2H, indole-NH), 7.88 (s, 3H, NH, NH, NH), 7.54 (d, 1H, *J* 7.6 Hz, H7''), 7.53 (d, 1H, *J* 7.5 Hz, H9'), 7.36 (d, 1H, *J* 7.6 Hz, H4''), 7.32 (d, 1H, *J* 7.6 Hz, H6'), 7.23 (d, 1H, *J* 2.3 Hz, H4'), 7.13 (d, 1H, *J* 2.3 Hz, H2''), 7.02 (m, 4H, H7', H8', H5'', H6''), 4.15 (m, 1H, H1'), 3.14 (dd, 1H, *J*₁ 4.0 Hz, *J*₂ 15.0 Hz H2b'), 3.07 (m, 2H, H10''), 2.98 (m, 2H, H9''), 2.87 (dd, 1H, *J*₁ 7.3 Hz, *J*₂ 14.9 Hz H2a'). ¹³C-NMR spectrum in DMSO-d₆ (δ, ppm): 185.2 (C1), 168.2 (C2), 136.8 (C3''), 136.5 (C5'), 127.8 (C8''), 127.3 (C10'), 124.1 (C2''), 123.9 (C4'), 121.6 (C5''), 121.3 (C7'), 118.9 (C7''), 118.8 (C9'), 118.7 (C6''), 118.5 (C8'), 112.0 (C4''), 111.7 (C6'), 109.8 (C1''), 109.6 (C3'), 61.0 (C1'), 31.1 (C10''), 27.4 (C2'), 23.6 (C9''). HRMS (ESI) *m/z*: 411.1907 [M + Na].

2.2.11 (S)-2-(tert-Butoxycarbonylamino)-3-(1H-indol-3-yl)propanoic acid (T1)

A solution mixture of L-tryptophan (20.45 g, 0.10 mol), sodium hydroxide pellets (8.80 g, 0.22 mol), and di-*tert*-butyl dicarbonate (24.01 g, 0.11 mol) in THF/H₂O (1:1)

100 mL was stirred at room temperature for 18 h. After the reaction was complete, water was added to dissolve the precipitate. Then, THF was removed under reduced pressure, and aqueous layer was extracted with dichloromethane. The aqueous layer was acidified by 1 N HCl to pH 4 and extracted with ethyl acetate. The organic phase was dried to yield white solid of compound **T1**. Yield 24.05 g (79%); m.p. 141–143 °C. ¹H-NMR spectrum in DMSO-d₆ (δ, ppm): 12.55 (s, 1H, COOH), 10.84 (s, 1H, indole NH), 7.53 (d, 1H, *J* 7.7 Hz, H9'), 7.34 (d, 1H, *J* 8.0 Hz, H6'), 7.15 (d, 1H, *J*₁ 1.5 Hz, H4'), 7.07 (t, 1H, *J* 7.4 Hz, H7'), 6.99 (t, 1H, *J* 7.14 Hz, H8'), 4.16 (m, 1H, H1'), 3.14 (dd, 1H, *J*₁ 4.5 Hz, *J*₂ 14.5 Hz, H2b'), 2.98 (dd, 1H, *J*₁ 9.4 Hz, *J*₂ 14.5 Hz, H2a'), 1.33 (s, 9 H, CH₃).

2.2.12 (S)-Methyl 2-((S)-2-amino-3-(1H-indol-3-yl)propano amido)-3-hydroxy propanoate (T2)

A solution of compound **T1** (304 mg, 1 mmol), L-serine methyl ester hydrochloride (155 mg, 1 mmol) HBTU (568.86 mg, 1.5 mmol), and DIPEA (0.42 mL, 3 mmol) in 5 mL of DMF was stirred at room temperature for 18 h. After the reaction was complete, water was added. The aqueous phase was extracted with ethyl acetate. The organic solution was dried over sodium sulphate, concentrated and purified by column chromatography on silica gel (EtOAc/hexane 4:1) to yield intermediated compound. Then, 10 mL of 1 N KOH in methanol was added to the obtained compound, and the reaction mixture was stirred at room temperature for 3 h. The reaction mixture was adjusted to pH 7 by 1 N HCl and extracted with ethyl acetate. The combined organic layers were dried to yield compound **T2** as white solid. Yield 267.05 mg (68.23%); m.p. 75–76 °C. ¹H-NMR spectrum in DMSO-d₆ (δ, ppm): 10.81 (s, 1H, indole NH), 8.20 (d, 1H, *J* 7.4 Hz, NH), 7.62 (d, 1H, *J* 7.7 Hz, H9'), 7.33 (d, 1H, *J* 7.8 Hz, H6'), 7.15 (s, 1H, H4'), 7.06 (t, 1H, *J* 7.5 Hz, H7'), 6.98 (t, 1H, *J* 7.4 Hz, H8'), 4.40 (m, 1H, H2), 4.28 (m, 1H, H1'), 3.75 (dd, 2H, *J*₁ 4.5 Hz, *J*₂ 10.8 Hz, H4), 3.11 (dd, 1H, *J*₁ 3.8 Hz, *J*₂ 14.6 Hz, 1H, H2b'), 2.91 (dd, 1H, *J*₁ 9.7 Hz, *J*₂ 14.7 Hz, H2a'), 1.30 (s, 9H, CH₃).

2.2.13 (S,Z)-tert-Butyl(6-((1H-indol-3-yl)methyl)-10,10-dimethyl-5,8-dioxo-9-oxa-2-thia-4,7-diazaundecan-3-ylidene)carbamate (T3)

A solution of compound **T1** (304 mg, 1 mmol), compound **1a** (160.22 mg, 1 mmol), HATU (570 mg, 1.5 mmol), and N-methylmorpholine (NMM) (0.22 mL, 2 mmol) in 5 mL

of DMF was stirred at room temperature for 18 h. After the reaction was complete, water was added and extracted with ethyl acetate. The organic solution was dried. The obtained residue was purified by column chromatography on silica gel (EtOAc/Hex 1:4) to yield compound **5** as white powder. Yield 324.77 mg (68.20%); m.p. 80–81 °C. ¹H-NMR spectrum in DMSO-d₆ (δ, ppm): 12.17 (s, 1H, NH), 10.85 (s, 1H, indole-NH), 7.49 (s, 1H, NH), 7.57 (d, 1H, *J* 7.75 Hz, H9'), 7.33 (d, 1H, *J* 8.0 Hz, H6'), 7.19 (d, 1H, *J* 1.7 Hz, H4'), 7.07 (t, 2H, *J* 7.0 Hz, H7'), 6.99 (t, 1H, *J* 7.0 Hz, H8'), 4.27 (m, 1H, H1'), 3.19 (dd, 1H, *J*₁ 4.8 Hz, *J*₂ 14.7 Hz, H2b'), 2.97 (dd, 1H, *J*₁ 9.8 Hz, *J*₂ 14.6 Hz, H2a'), 2.30 (s, 3H, CH₃), 1.45 (s, 9H, CH₃), 1.33 (s, 9H, CH₃).

2.2.14 *N*-tert-Butoxycarbonyl (Boc)-protected 2-methyl-2-thiopseudourea (**1a**)

A solution of methylisothiurea hemisulfate salt (198 mg, 1 mmol) in THF/H₂O (1:1) 30 mL was added with sodium bicarbonate (168 mg, 1 mmol), di-*tert*-butyl dicarbonate (218 mg, 1 mmol), and stirred at room temperature for 18 h. After the reaction was complete, THF was removed under reduced pressure, and aqueous layer was extracted with dichloromethane. The organic phase was dried to yield compound **1a** as colorless viscous liquid. Yield 195.71 mg (76.62%). ¹H-NMR spectrum in DMSO-d₆ (δ, ppm): 8.54 (s, 1H, NH), 2.31 (s, 3H, CH₃), 1.40 (s, 9H, CH₃).

2.3 Biological experiment part

BACE1 enzyme and the BACE1 substrate were purchased from Sino Biological® and Calbiochem®, respectively. Aβ (1–42) from Anaspec® was used in the ThT assay. IC₅₀ values were calculated using GraphPad Prism 4 with nonlinear regression curve fit. Statistics were determined by ANOVA, calculated using IBM SPSS statistics version 24.

2.3.1 BACE1 inhibition assay

The test compound, prepared at various concentrations in 5% DMSO, was added to black 96 well plates followed by 30 μl of enzyme working solution (0.01 unit/μl) and 20 μl of substrate solution (125 μM). The final volume was adjusted to 100 μl with 100 mM sodium acetate buffer (pH 4.5), and the reaction plate was incubated at

37°C for 30 min. The emitted fluorescence (*E*_m) was measured at 510 nm after excitation (*E*_x) at 380 nm [15]. Compound **12c**, previously synthesized and described in [16], was used as an in house BACE1 inhibitor positive control at a final concentration of 100 μM. The resulting data were analyzed, and compounds showing greater than 70% inhibition were evaluated at concentrations of 5–25 μM to determine their IC₅₀ values. The IC₅₀ values were calculated using GraphPad Prism 4 with a nonlinear regression curve fit.

2.3.2 Aβ aggregation inhibition assay

Amyloid solution in 50 mM Tris buffer (pH 7.4) at a concentration of 25 μM (9 μL) was added to transparent 96 well plate followed by test compounds (1 μL) at various concentrations prepared in DMSO. The reaction was mixed gently by tapping and incubated in dark at 37°C for 48 h. After incubation, 200 μL of 5 μM thioflavin-T (Sigma®) in 50 mM Tris buffer (pH 7.4) was added to each well. The emitted fluorescence (*E*_m) was measured at 490 nm after excitation (*E*_x) at 446 nm [17]. Curcumin was included in the assay as a positive control. The resulting data were analyzed and compounds showing more than 70% inhibition were evaluated to determine their IC₅₀ values. The data were analyzed using GraphPad Prism 4 with a nonlinear regression curve fit.

2.3.3 Antioxidant assay

The test compounds were prepared at a concentration of 500 μM in 50% DMSO. DPPH, prepared at a concentration of 500 μM in methanol, was added to transparent 96 well plates in a volume of 70 μL per well. Methanol was used to adjust the volume to 80 μL. After adjusting the volume, 20 μL of test compound was added to each well. The reaction plate was incubated at room temperature in dark for 30 min. The absorption was measured at wavelength 517 nm [18]. Ascorbic acid was used as a positive control. The percent inhibition was calculated. Compounds showing inhibition greater than 70% were evaluated to determine their IC₅₀ values.

2.3.4 Neuroprotective effect on β-amyloid-induced cell damage

Protective effect on β-amyloid-induced cell damage was evaluated in human neuroblastoma cell (SH-SY5Y) cells.

SH-SY5Y cells were cultured in Ham's F12:Dulbecco's modified Eagle's medium (DMEM) containing 50 IU/mL penicillin, 50 g/mL streptomycin, 2 mM L-glutamine, and 10% fetal bovine serum. Cell cultures were maintained at 37°C in an atmosphere of 95% humidified air and 5% CO₂. For the assays, SH-SY5Y cells were sub-cultured into a 96-well plate for 24 h. The cells were then incubated with Aβ₁₋₄₂ (25 μM) with or without various concentrations of the test compounds for 24 h. Curcumin at a concentration of 10 μM was used as positive control. Cell viability was determined by staining the cells using water-soluble tetrazolium salt (WST-8) assay. The absorption was measured using a well plate reader at 450 nm [19].

Ethical approval: The conducted research is not related to either human or animal use.

3 Results and discussion

3.1 Design and docking study

Tryptophan was designed to be the core structure due to its properties in blood brain penetration via the large neutral amino acid transporter 1 or LAT1 transporter [20,21] and the BACE1 inhibitory activity [11]. The modification of the tryptophan was designed by including aromatic systems substituted with nucleophilic groups, such as hydroxyl groups, into the moieties based on reported pharmacophore models of anti-amyloid aggregation, antioxidant and metal chelating properties [22,23]. The proposed of extended part is to enhance the binding affinity for BACE1 in order to access the S3 pocket and also to contribute to multifunctional properties.

The expanded moiety was composed of two parts: R1 and R2. The amino acid (R1) was designed as a linker which contained a hydrogen bond acceptor to enable additional hydrogen bonding with Asp32 or Asp228, the key catalytic residues in BACE1 (Figure 1). Thus, amino acids with side chains bearing hydrogen bond donor such as –OH and –NH–, serine, tyrosine, threonine, and guanidine were selected as R1 linkers. The R2 terminal of the expanded moiety was designed to be an aromatic system with a nucleophilic motif to provide antioxidant activity. Moreover, the number of carbon atoms between the amino acid linker, R1, and the aromatic terminal R2 was varied between 7 and 10 Å, considering the optimal 8–9 Å distance when binding to Aβ (Figure 1) [22]. All 16 designed compounds were screened *in silico* with the main target BACE1, 2IRZ-F template, using the AutoDock program suite, version 4.2, to identify hit compounds for synthesis. The docking results were showed in Table 1.

The docking results showed that compounds in the TSR and TGN series generally gave better binding results than those in TYR and TTH series. This was because their binding mode allowed the linker R1 (serine or guanidine) to form extra H-bonds with the catalytic residues, Asp32 or Asp228. Moreover, ligand efficiency (LE) values and free binding energy of the four compounds in the TYR series with tyrosine as the linker (LE: –0.26 to –0.30 and ΔG: –9.1 to –10.0 kcal/mol) were not as favorable as those of the compounds in the TSR (LE: –0.38 to –0.43 and ΔG: –11.5 to –12.5 kcal/mol) or TGN series (LE: –0.44 to –0.48 and ΔG: –11.7 to –14.0 kcal/mol). The inferior binding affinity of the compounds in the TYR series was possibly due to their steric properties and greater flexibility of the tyrosine side chain. Compounds in the TTH series also presented good LE values and binding affinities, however, the linker R1 could not form an extra H-bond with the key residues Asp32 or Asp228. Therefore, compounds in the TYR and TTH series were not included in the synthesis part of the study.

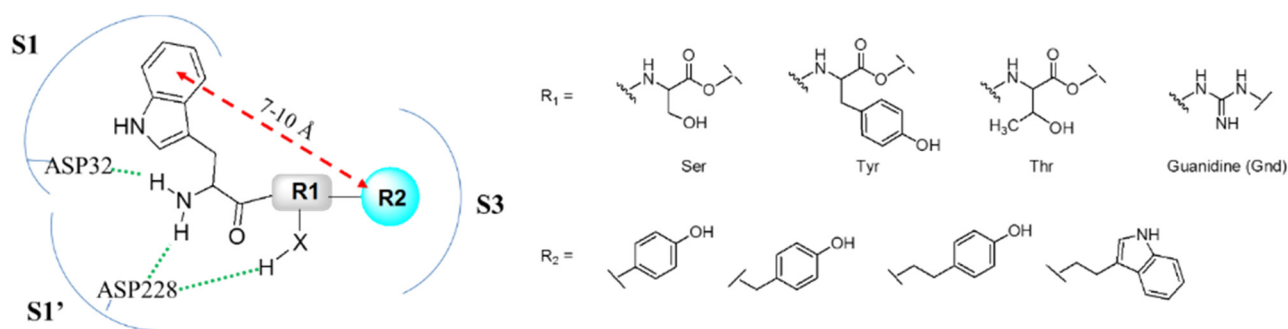
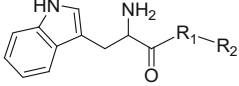
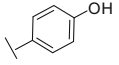
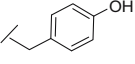
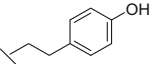
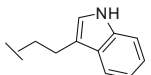
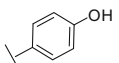
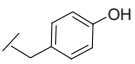
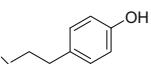
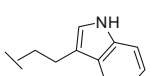
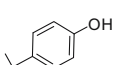
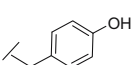
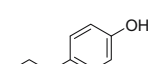
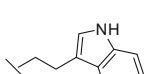
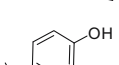
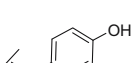
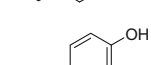
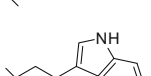


Figure 1: The proposed designed compounds (X = O or N atom).

Table 1: Docking results of the designed compounds against the BACE1 template

| Cpd | R ₁ | R ₂ | ΔG (kcal/mol) | LE ^a | H-bond number | H-bond interacting residues (distance, Å) |
|------|----------------|---|--------------------------|-----------------|------------------|---|
| | | | | | | |
| | |  | | | | |
| TSR1 | Ser |  | -11.5 | -0.41 | 6 | Asp32 (1.8), Gln73 (2.0), Asp228 (1.9, 2.0), Thr231 (1.9, 1.9) |
| TSR2 | Ser |  | -12.5 | -0.43 | 6 | Asp32 (1.7), Ser36 (1.9), Asn37 (1.9), Thr73 (2.1), Tyr198 (2.2), Asp228 (2.0) |
| TSR3 | Ser |  | -11.8 | -0.39 | 7 | Asp32 (1.7), Ser35 (2.0), Asn37 (1.9), Gln73 (2.3), Asp228 (1.9, 1.9), Thr231 (2.2) |
| TSR4 | Ser |  | -11.8 | -0.38 | 4 | Asp32 (1.9), Asp228 (1.8, 1.9), Thr231 (2.1) |
| TYR1 | Tyr |  | -9.1 | -0.26 | 5 | Gly34 (2.1), Gln73 (2.1), Phe108 (2.5), Thr231 (2.0), Thr232 (2.0) |
| TYR2 | Tyr |  | -10.5 | -0.30 | 4 | Asp32 (1.8), Ser229 (2.1), Gly230 (2.0), Thr232 (2.1) |
| TYR3 | Tyr |  | -10.3 | -0.28 | 3 | Phe108 (2.0), Gly230 (2.0), Thr231 (2.5) |
| TYR4 | Tyr |  | -10.0 | -0.26 | 4 | Gln73 (1.9), Gly230 (2.0), Thr231 (2.2), Thr232 (2.0) |
| TTH1 | Thr |  | -11.6 | -0.40 | 4 | Asp32 (1.9), Gln73 (1.9), Asp228 (1.8), Thr231 (2.1) |
| TTH2 | Thr |  | -12.5 | -0.41 | 5 | Asp32 (1.6), Ser35 (2.0), Thr72 (2.3), Asn73 (2.1), Asp228 (1.9) |
| TTH3 | Thr |  | -12.7 | -0.40 | 6 | Asp32 (1.6), Ser35 (1.7), Thr72 (2.4), Asn73 (2.0), Asp228 (1.8), Thr231 (2.0) |
| TTH4 | Thr |  | -13.0 | -0.39 | 5 | Asp32 (1.7), Thr72 (2.1), Gln73 (2.0), Asp228 (1.8), Gly230 (2.0) |
| TGN1 | Gnd |  | -11.7 | -0.47 | 5 | Asp32 (1.9), Asp228 (1.7, 2.2), Thr72 (2.1), Thr232 (2.1) |
| TGN2 | Gnd |  | -12.3 | -0.47 | 5 | Asp32 (1.7, 2.0), Thr72 (2.2), Asp228 (2.0), Thr232 (1.9) |
| TGN3 | Gnd |  | -12.0 | -0.44 | 6 | Asp32 (1.8), Thr72 (2.1), Asp228 (1.7, 2.1), Thr231 (1.9), Ser325 (2.0) |
| TGN4 | Gnd |  | -14.0 | -0.48 | 3 | Asp32 (1.7), Asp228 (1.7), Gly230 (1.9) |

^aLE = $\Delta G/N$, N is number of nonhydrogen atom.

3.2 Multifunctional assay

The compounds in the TSR and TGN series were initially screened for their inhibitory actions against BACE1, anti-amyloid aggregation effects, and antioxidant properties at a concentration of 100 μM , and the screening results are shown in Table 2. Compounds that demonstrated a percentage inhibition greater than 70% were further evaluated to determine their IC_{50} values. Positive controls for each assay were performed at the same concentration.

3.2.1 BACE1 inhibition assay

TSR2, **TSR4**, and **TGN2** were found to be the potent inhibitors of BACE1. The IC_{50} values of these compounds were in the range of 21.38–24.18 μM . The binding modes of the three compounds are shown in Figure 2. The amino group in the tryptophan core structure of these three compounds provided H-bonds with the catalytic residues Asp32 and Asp228, and the compounds were well accommodated in binding pockets to form 5–6 hydrogen bonds. The OH of the serine and the NH of the guanidine linker did not form hydrogen bonds with the catalytic amino acids as expected, instead the NH of the amide backbone of both **TSR4** and **TGN2** formed additional H-bonds with Asp32 and Asp228. Moreover, the OH of the serine linker in compound **TSR4** formed an H-bond with Thr231. The indole in the tryptophan core of compounds **TSR2** and **TSR4** was anchored to the S1 binding pocket whereas the middle part of **TSR2** binding pose was aligned in the same

orientation as **TGN2**. However, the tryptophan cores of **TSR2** and **TGN2** flipped into the opposite direction, the phenolic end (R_2) of **TSR2** directed to the S2'/S3' pocket, providing H-bonding and hydrophobic interactions with residues in these pockets. The access to the S2'/S3' pocket accommodated the phenolic OH and the NH between the middle serine and the phenolic group of **TSR2** to form three hydrogen bonds with Ser36, Asn37, and Tyr198 (Figure 2b). Moreover, the insertion of the phenolic moiety of **TSR2** contributed to interactions with the residues in the S3' pocket, especially with Arg128, the amino acid reported to affect the binding conformation of a potent inhibitor (Figure 2b) [13]. These interactions enabled **TSR2** to achieve the same level of inhibition as **TSR4** and **TGN2**, although it was inaccessible to the S3 pocket.

3.2.2 A β aggregation inhibition assay

The anti-A β aggregation screening results obtained at a concentration of 100 μM showed that compounds **TSR1**, **TSR2**, and **TGN2** inhibited amyloid aggregation by more than 70% (Table 2), and the IC_{50} values of these compounds were 38.55 μM , 37.06 μM , and 36.12 μM , respectively. The distances between aromatic terminals in the docked poses of compounds **TSR1**, **TSR2**, and **TGN2** were measured and found to be 8.50 Å, 9.88 Å, and 8.00 Å, respectively, which are within the theoretical optimal distance (8–9 Å) [22]. The binding mode of the lead compounds with A β template revealed that **TSR1**-formed H-bonds with Glu11 (1.78 Å), Gln15

Table 2: Multifunctional activity of TSR and TGN compounds

| Compounds | BACE1 inhibition | | Anti-amyloid aggregation | | Antioxidant | |
|-----------------------|--|------------------------------------|--|------------------------------------|--|------------------------------------|
| | % inhibition at 100 μM (\pm SD) | IC_{50} (μM) | % inhibition at 100 μM (\pm SD) | IC_{50} (μM) | % inhibition at 100 μM (\pm SD) | IC_{50} (μM) |
| TSR1 | 50.64 (\pm 0.72)* | — | 88.06 (\pm 1.22)* | 38.55 | 15.36 (\pm 0.66)* | — |
| TSR2 | 88.07 (\pm 2.87) | 24.18 | 73.15 (\pm 0.50)* | 37.06 | 4.28 (\pm 1.02)* | — |
| TSR3 | 46.72 (\pm 2.12)* | — | 53.33 (\pm 1.85)* | — | 3.47 (\pm 0.81)* | — |
| TSR4 | 96.98 (\pm 1.62)* | 21.38 | 46.32 (\pm 1.23)* | — | 9.78 (\pm 0.66)* | — |
| TGN1 | 49.60 (\pm 2.33)* | — | 36.12 (\pm 0.51)* | — | 81.88 (\pm 0.45)* | 36.14 |
| TGN2 | 94.35 (\pm 1.86) | 22.35 | 86.96 (\pm 0.82) | 36.12 | 13.05 (\pm 1.45)* | — |
| TGN3 | 99.68 (\pm 1.02) | 31.03 | 54.32 (\pm 2.35)* | — | 16.38 (\pm 0.67)* | — |
| TGN4 | 85.65 (\pm 0.15) | 35.35 | 49.78 (\pm 1.54)* | — | 8.19 (\pm 1.39)* | — |
| BACE1 inhibitor (12c) | 92.64 (\pm 1.72) | 20.89 | — | — | — | — |
| Curcumin | — | — | 84.02 (\pm 1.07) | 0.63 | — | — |
| Ascorbic acid | — | — | — | — | 54.16 (\pm 0.77) | 94.92 |

Data are mean \pm SD ($n = 3$), * p value < 0.001 compared with the positive control of each group (paired t -test statistic from Microsoft Excel). Structure of positive control compounds was shown in the supplemental information (Figures S21 and S22).

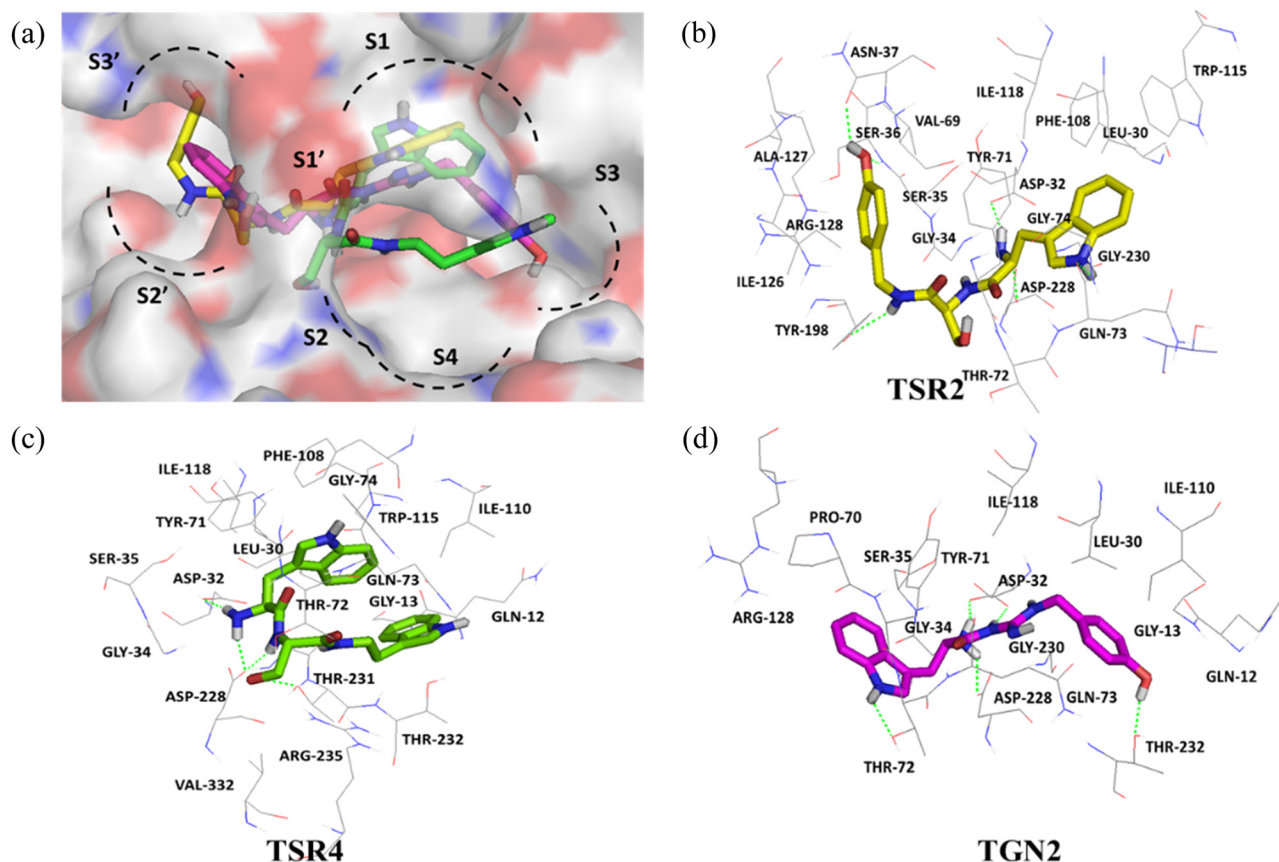


Figure 2: The binding modes of **TSR2** (yellow), **TSR4** (green), and **TGN2** (magenta) in the active binding site of BACE1, overlay of docked poses (a); and the interacting residues, showing hydrogen bonds as green dotted lines (b–d).

(2.09 Å), Glu22 (1.86 Å) and Asp23 (2.01 Å), while **TSR2** provided H-bonds with Glu22 (1.92, 1.94 and 2.11 Å) and Asp23 (1.86 Å) (Figure 3a). The potent inhibitory activity of **TSR1** and **TSR2** against amyloid aggregation was possibly a result of two crucial types of interactions, H-bond interactions and hydrophobic interactions, with

the key residues responsible for self-binding and the oligomer formation leading to aggregation.

H-bond interactions have been detected, particularly with Asp23, which is the key amino acid for intermolecular salt bridge formation of A β peptides in protein aggregation [24,25]. Hydrophobic interactions have been

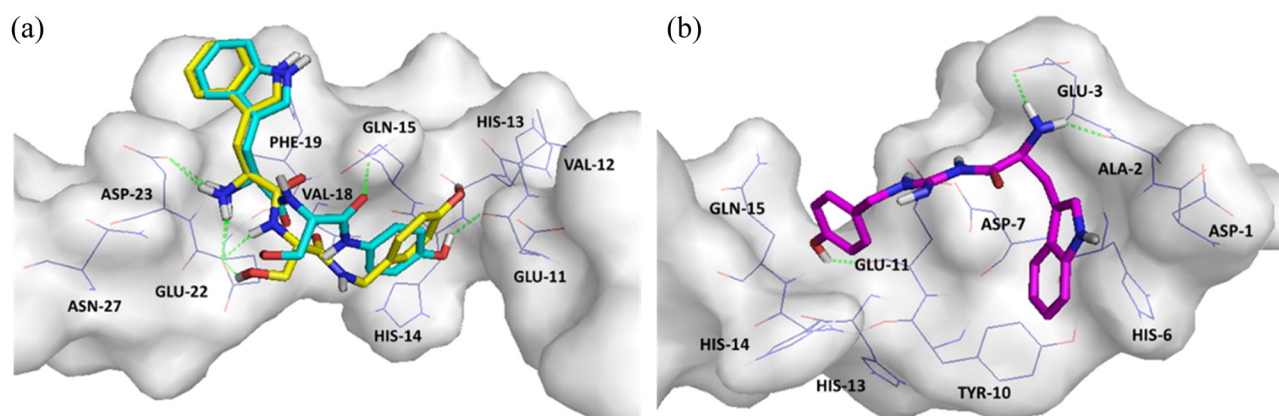


Figure 3: The binding modes of the lead compounds with A β peptide: (a) **TSR1** (cyan) and **TSR2** (yellow); (b) **TGN2** (magenta).

found with the key residue Phe19, the amino acid in the hydrophobic interaction region [25] that connects two β -strands of A β monomers, in the initiation of oligomer and fibril formation [26]. Thus, ligand binding with these amino acid residues (Phe19 and Asp23) was a contributing factor to the blocking of A β oligomer formation and hence to anti-aggregation activity. Besides Phe19 and Asp23, **TSR1** and **TSR2** were found to interact with His13 and His14, in the metal-binding site [27]. The metal-binding site (His6, His13, and His14) has been reported as the part of two monomers that coordinate with a metal ion (Cu^{2+} or Zn^{2+}) [28,29]. This metal binding stabilizes and increases amyloid oligomerization [28,30]. Compound **TGN2** formed H-bond interactions with Ala2 (1.74 Å), Glu3 (1.94 Å), and Glu11 (1.85 Å) (Figure 3b). Hydrophobic interactions of **TGN2** were also found with all key amino acid residues in the metal-binding site, His6, His13, and His14 [31]. Moreover, all three compounds also had hydrophobic interactions with Gln15 and Val18, which are self-recognition residues in the aggregation process [32]. Taken together, binding at the important regions responsible for A β aggregation, namely, the hydrophobic region, the intermolecular salt bridge, and the metal-binding site resulted in the enhancement of anti-amyloid aggregation activity in the tested compounds.

3.2.3 Antioxidant assay

The antioxidant activity of the hit compounds was evaluated at concentrations of 100 μM using the DPPH

scavenging method [18]. **TGN1** was the only compound that showed high inhibition, with IC_{50} values of 36.14 μM , approximately three times better than that of ascorbic acid (IC_{50} 94.92 μM). The direct guanidine substitution at the *para*-position of the phenol group in **TGN1** might be the reason for its antioxidant properties, because of its strong electron-donating group via the π -bond and increased number of conjugated double bonds in the **TGN1** molecule [33,34].

3.2.4 Neuroprotective effect on β -amyloid-induced cell damage

Among the eight compounds, two compounds, **TSR2** and **TGN2**, possessed dual activities. **TSR2** and **TGN2** were evaluated for their neuroprotective effects on A β -induced cytotoxicity in SH-SY5Y neuroblastoma cells. The cytotoxicity of **TSR2** and **TGN2** was initially tested at 1, 10, and 100 $\mu\text{g}/\text{mL}$ by the MTT assay. No significant reduction in cell viability was found at any of the tested concentrations, which indicated nontoxicity at the highest concentration (100 $\mu\text{g}/\text{mL}$). **TSR2** and **TGN2** were then screened at the highest concentration (100 $\mu\text{g}/\text{mL}$) for neuroprotective effects with the WST-8 assay, in which A β 1–42 (25 μM) was used to induce cytotoxicity in SH-SY5Y cells. Cell viability was determined by measuring the absorption of the WST-8 at 450 nm [19]. The screening results are shown in Figure 4a. Neither compound showed neuroprotection at 100 $\mu\text{g}/\text{mL}$ as anticipated, instead they presented lower percentage viability than the A β -treated group.

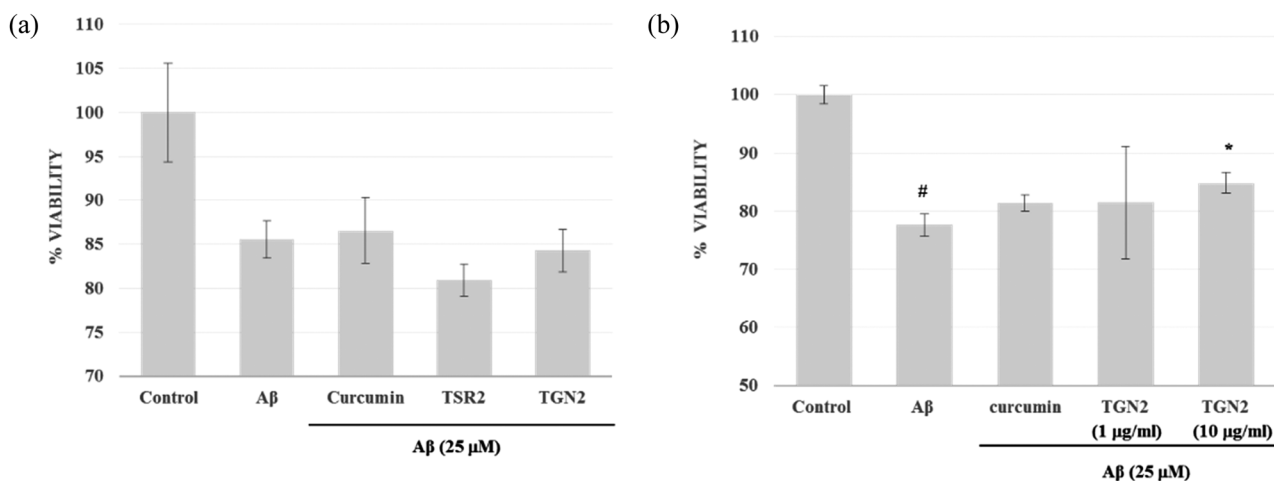


Figure 4: Neuroprotective effects of dual activity compound against A β induced cytotoxicity: (a) the screening results at the nontoxic concentration of 100 $\mu\text{g}/\text{mL}$; (b) neuroprotective effects of **TGN2**. Data are mean \pm SD ($n = 3$), # $p < 0.01$ compared with the control group and * $p < 0.01$ compared with the A β -treated group (paired t -test statistic from Microsoft Excel).

Although **TSR2** and **TGN2** alone were nontoxic at 100 μM , it is likely that a synergistic effect occurred with the combination of $\text{A}\beta$ and the test compounds at this concentration. As the percentage viability of **TGN2** treated cells was slightly lower than that of $\text{A}\beta$ treated cells, **TGN2** was tested at lower doses (1 $\mu\text{g}/\text{mL}$ and 10 $\mu\text{g}/\text{mL}$) to avoid the synergistic effect. **TGN2** at lower concentrations appeared to reduce the cytotoxicity of $\text{A}\beta$ (Figure 4b). However, a significant neuroprotective effect was observed only at 10 $\mu\text{g}/\text{mL}$ or 2.62 μM .

4 Conclusion

Among the developed compounds, **TGN2** was found to exhibit multifunctionality, with potent actions as a BACE1 inhibitor and against amyloid aggregation. **TGN1** was found as a potent antioxidant with greater activity than ascorbic acid. Moreover, based on its multifunctional activity on the $\text{A}\beta$ cascade, **TGN2** at a concentration of 2.62 μM showed a significant neuroprotective effect against $\text{A}\beta$ -induced cytotoxicity.

Conflict of interest: The authors have declared no conflict of interest.

Acknowledgments: The authors would like to acknowledge the financial support from the Office of the High Education Commission and Mahidol University under the National Research Universities and the Commission on Higher Education (grant number CHE-RG-2551-53). This research work was partially supported by Chiang Mai University.

References

- [1] Barage SH, Sonawane KD. Amyloid cascade hypothesis: pathogenesis and therapeutic strategies in Alzheimer's disease. *Neuropeptides*. 2015;52:1–18. doi: 10.1016/j.npep.2015.06.008
- [2] Klafki HW, Staufienbiel M, Kornhuber J, Wiltfang J. Therapeutic approaches to Alzheimer's disease. *Brain*. 2006;129(11):2840–55. doi: 10.1093/brain/awl280
- [3] Ghosh AK, Osswald HL. BACE1 (β -secretase) inhibitors for the treatment of Alzheimer's disease. *Chem Soc Rev*. 2014;43(19):6765–813. doi: 10.1039/c3cs60460h
- [4] Nie Q, Du XG, Geng MY. Small molecule inhibitors of amyloid β peptide aggregation as a potential therapeutic strategy for Alzheimer's disease. *Acta Pharm Sin*. 2011;32(5):545–51. doi: 10.1038/aps.2011.14
- [5] Imbimbo BP. Therapeutic potential of gamma-secretase inhibitors and modulators. *Curr Top Med Chem*. 2008;8(1):54–61. doi: 10.2174/156802608783334015
- [6] Cummings J, Lee G, Mortsdorf T, Ritter A, Zhong K. Alzheimer's disease drug development pipeline: 2017. *Alzheimers Dement*. 2017;3(3):367–84. doi: 10.1016/j.trci.2017.05.002
- [7] Luo XT, Wang CM, Liu Y, Huang ZG. New multifunctional melatonin derived benzylpyridinium bromides with potent cholinergic, antioxidant, and neuroprotective properties as innovative drugs for Alzheimer's disease. *Eur J Med Chem*. 2015;103:302–11. doi: 10.1016/j.ejmech.2015.08.052
- [8] Xie SS, Wang X, Jiang N, Yu W, Wang KDG, Lan JS, et al. Multi-target tacrine-coumarin hybrids: cholinesterase and monoamine oxidase B inhibition properties against Alzheimer's disease. *Eur J Med Chem*. 2015;95:153–65. doi: 10.1016/j.ejmech.2015.03.040
- [9] Estrada M, Herrera-Arozamena C, Pérez C, Viña D, Romero A, Morales-García JA, et al. New cinnamic – *N*-benzylpiperidine and cinnamic – *N,N*-dibenzyl(*N*-methyl)amine hybrids as Alzheimer-directed multitarget drugs with antioxidant, cholinergic, neuroprotective and neurogenic properties. *Eur J Med Chem*. 2016;121:376–86. doi: 10.1016/j.ejmech.2016.05.055
- [10] Barar J, Rafi MA, Pourseif MM, Omid Y. Blood-brain barrier transport machineries and targeted therapy of brain diseases. *Bioimpacts*. 2016;6(4):225–48. doi: 10.15171/bi.2016.30
- [11] Jiaranaikulwanitch J, Boonyarat C, Fokin VV, Vajragupta O. Triazolyl tryptoline derivatives as β -secretase inhibitors. *Bioorg Med Chem Lett*. 2010;20(22):6572–6. doi: 10.1016/j.bmcl.2010.09.043
- [12] Rajapakse HA, Nantermet PG, Selnick HG, Munshi S, McGaughey GB, Lindsley SR, et al. Discovery of oxadiazoyl tertiary carbinamine inhibitors of beta-secretase (BACE-1). *J Med Chem*. 2006;49(25):7270–3. doi: 10.1021/jm061046r
- [13] Hong L, Koelsch G, Lin X, Wu S, Terzyan S, Ghosh AK, et al. Structure of the protease domain of memapsin 2 (beta-secretase) complexed with inhibitor. *Science*. 2000;290(5489):150–3. doi: 10.1126/science.290.5489.150
- [14] Tomaselli S, Esposito V, Vangone P, van Nuland NAJ, Bonvin AM, Guerrini R, et al. The α -to- β conformational transition of Alzheimer's $\text{A}\beta$ -(1–42) peptide in aqueous media is reversible: a step by step conformational analysis suggests the location of β conformation seeding. *ChemBioChem*. 2006;7(2):257–67. doi: 10.1002/cbic.200500223
- [15] Ermolieff J, Loy JA, Koelsch G, Tang J. Proteolytic activation of recombinant Pro-memapsin 2 (Pro- β -secretase) studied with new fluorogenic substrates. *Biochemistry*. 2000;39(40):12450–6. doi: 10.1021/bi001494f
- [16] Jiaranaikulwanitch J, Govitrapong P, Fokin VV, Vajragupta O. From BACE1 inhibitor to multifunctionality of tryptoline and tryptamine triazole derivatives for Alzheimer's disease. *Molecules*. 2012;17(7):8312–33. doi: 10.3390/molecules17078312
- [17] LeVine 3rd H. Thioflavine T interaction with synthetic Alzheimer's disease beta-amyloid peptides: detection of amyloid aggregation in solution. *Protein Sci*. 1993;2(3):404–10. doi: 10.1002/pro.5560020312
- [18] Sharma OP, Bhat TK. DPPH antioxidant assay revisited. *Food Chem*. 2009;113(4):1202–5. doi: 10.1016/j.foodchem.2008.08.008
- [19] Thirattmatrakul S, Yenjai C, Waiwut P, Vajragupta O, Reubroycharoen P, Tohda M, et al. Synthesis, biological evaluation and molecular modeling study of novel

- tacrinecarbazole hybrids as potential multifunctional agents for the treatment of Alzheimer's disease. *Eur J Med Chem.* 2014;75:21–30. doi: 10.1016/j.ejmech.2014.01.020
- [20] Tarlunganu DC, Deliu E, Dotter CP, Kara M, Janiesch PC, Scalise M, et al. Impaired amino acid transport at the blood brain barrier is a cause of autism spectrum disorder. *Cell.* 2016;167(6):1481–94. doi: 10.1016/j.cell.2016.11.013
- [21] Rautio J, Gynther M, Laine K. LAT1-mediated prodrug uptake: a way to breach the blood–brain barrier? *Ther Deliv.* 2013;4(3):281–4. doi: 10.4155/tde.12.165
- [22] Reinke AA, Gestwicki JE. Structure–activity relationships of amyloid beta-aggregation inhibitors based on curcumin: influence of linker length and flexibility. *Chem Biol Drug Des.* 2007;70(3):206–15. doi: 10.1111/j.1747-0285.2007.00557.x
- [23] Geldenhuys WJ, Youdim MB, Carroll RT, Van, der Schyf CJ. The emergence of designed multiple ligands for neurodegenerative disorders. *Prog Neurobiol.* 2011;94(4):347–59. doi: 10.1016/j.pneurobio.2011.04.010
- [24] Lührs T, Ritter C, Adrian M, Riek-Loher D, Bohrmann B, Döbeli H, et al. 3D structure of Alzheimer's amyloid- β (1–42) fibrils. *Proc Natl Acad Sci U S A.* 2005;102(48):17342–7. doi: 10.1073/pnas.0506723102
- [25] Hayne DJ, Lim S, Donnelly PS. Metal complexes designed to bind to amyloid-[small beta] for the diagnosis and treatment of Alzheimer's disease. *Chem Soc Rev.* 2014;43:6701–15. doi: 10.1039/C4CS00026A
- [26] Alies B, Conte-Daban A, Sayen S, Collin F, Kieffer I, Guillon E, et al. Zinc(II) binding site to the Amyloid- β peptide: insights from spectroscopic studies with a wide series of modified peptides. *Inorg Chem.* 2016;55(20):10499–509. doi: 10.1021/acs.inorgchem.6b01733
- [27] Rezaei-Ghaleh N, Giller K, Becker S, Zweckstetter M. Effect of zinc binding on β -amyloid structure and dynamics: implications for A β aggregation. *Biophys J.* 2011;101(5):1202–11. doi: 10.1016/j.bpj.2011.06.062
- [28] Miller Y, Ma B, Nussinov R. Metal binding sites in amyloid oligomers: complexes and mechanisms. *Coord Chem Rev.* 2012;256(19–20):2245–52. doi: 10.1016/j.ccr.2011.12.022
- [29] Gaggelli E, Grzonka Z, Kozłowski H, Migliorini C, Molteni E, Valensin D, et al. Structural features of the Cu(II) complex with the rat A β (1–28) fragment. *Chem Commun.* 2008;2008:341–3. doi: 10.1039/b713453c
- [30] Miura T, Suzuki K, Kohata N, Takeuchi H. Metal binding modes of Alzheimer's amyloid β -peptide in insoluble aggregates and soluble complexes. *Biochemistry.* 2000;39(23):7024–31. doi: 10.1021/bi0002479
- [31] Kozin SA, Mezentsev YV, Kulikova AA, Indeykina MI, Golovin AV, Ivanov AS, et al. Zinc-induced dimerization of the amyloid-[small beta] metal-binding domain 1–16 is mediated by residues 11–14. *Mol Biosyst.* 2011;7(4):1053–5. doi: 10.1039/c0mb00334d
- [32] Ahmed M, Davis J, Aucoin D, Sato T, Ahuja S, Aimoto S, et al. Structural conversion of neurotoxic amyloid- β 1–42 oligomers to fibrils. *Nat Struct Mol Biol.* 2010;17(5):561–7. doi: 10.1038/nsmb.1799
- [33] Ji HF. Insight into the strong antioxidant activity of deinoxanthin, a unique carotenoid in *deinococcus radiodurans*. *Int J Mol Sci.* 2010;11(11):4506–10. doi: 10.3390/ijms11114506
- [34] Bendary E, Francis RR, Ali HMG, Sarwat MI, El Hady S. Antioxidant and structure–activity relationships (SARs) of some phenolic and anilines compounds. *Ann Agric Sci.* 2013;58(2):173–81. doi: 10.1016/j.aosas.2013.07.002